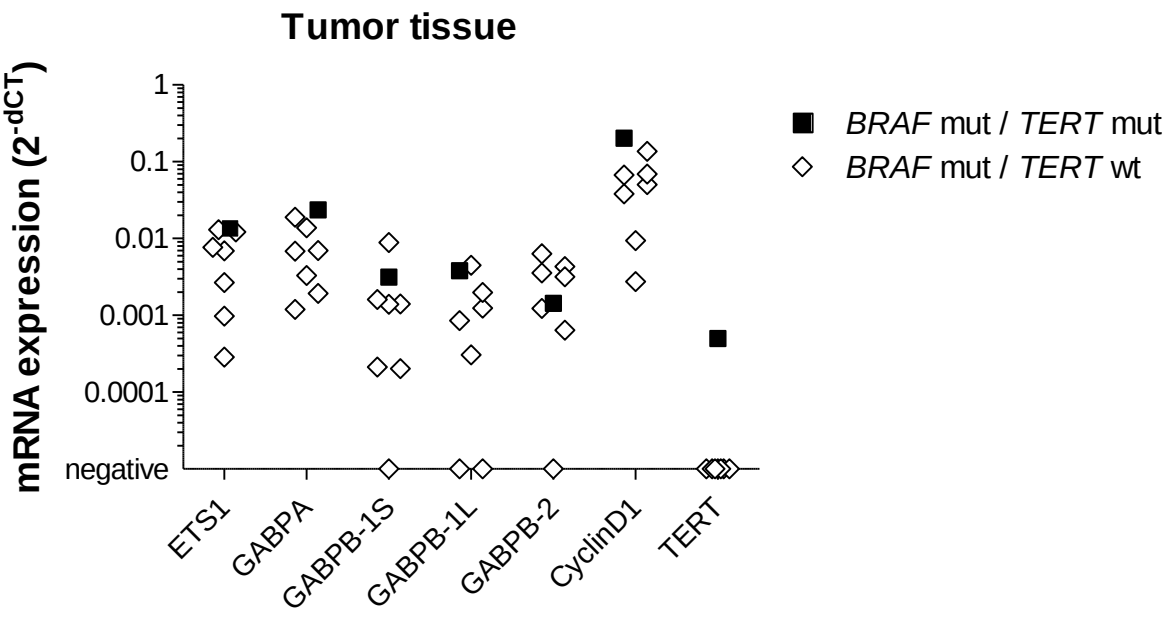

Figure S1. mRNA expression of ETS transcription factors and downstream targets in tumor tissue. mRNA expression of *ETS1, GABPA, GABPB-1S, GABPB-1L and GABPB-2*, as well as of ETS downstream targets *cyclin D1* and *TERT* was assessed using qRT-PCR. Expression was analyzed in tissues of one *BRAF* mut and *TERT* promoter-mut and seven *BRAF* mut/*TERT* promoter-wt glioma patients as indicated. Values are derived from triplicates and given as mean -dCT from *RPL-41* serving as internal control. wt = wild-type, mut = mutant

Gabler et al., supplementary figure 2

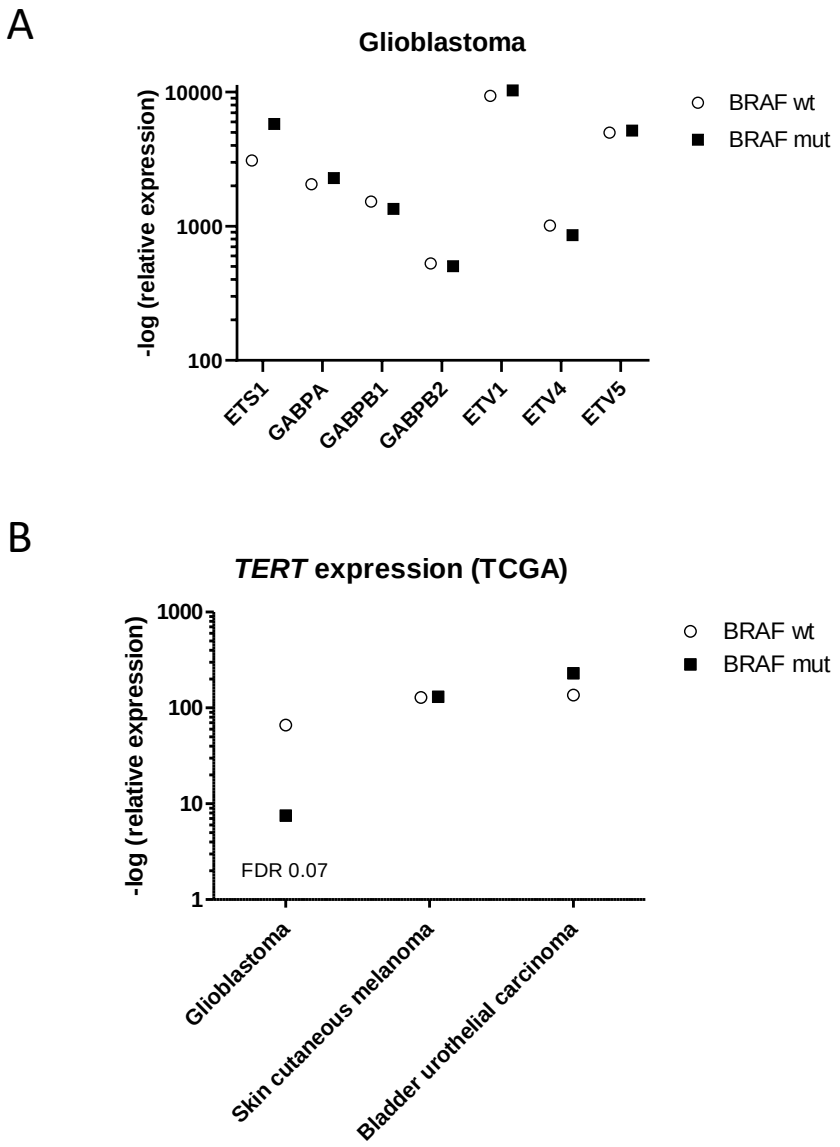

Figure S2. Expression of Ets-factors and *TERT* in TCGA RNA sequencing data sets. Average logarithmic relative Ets-factor **(A)** and *TERT* **(B)** expression in different tumor types stratified for *BRAF* mutation status as calculated by the respective RNA sequencing analysis algorithms (DESeq2). TCGA = The Cancer Genome Atlas, FDR, false discovery rate, wt = wild-type, mut = mutated, Source: TCGA data base

Gabler et al., supplementary figure 3

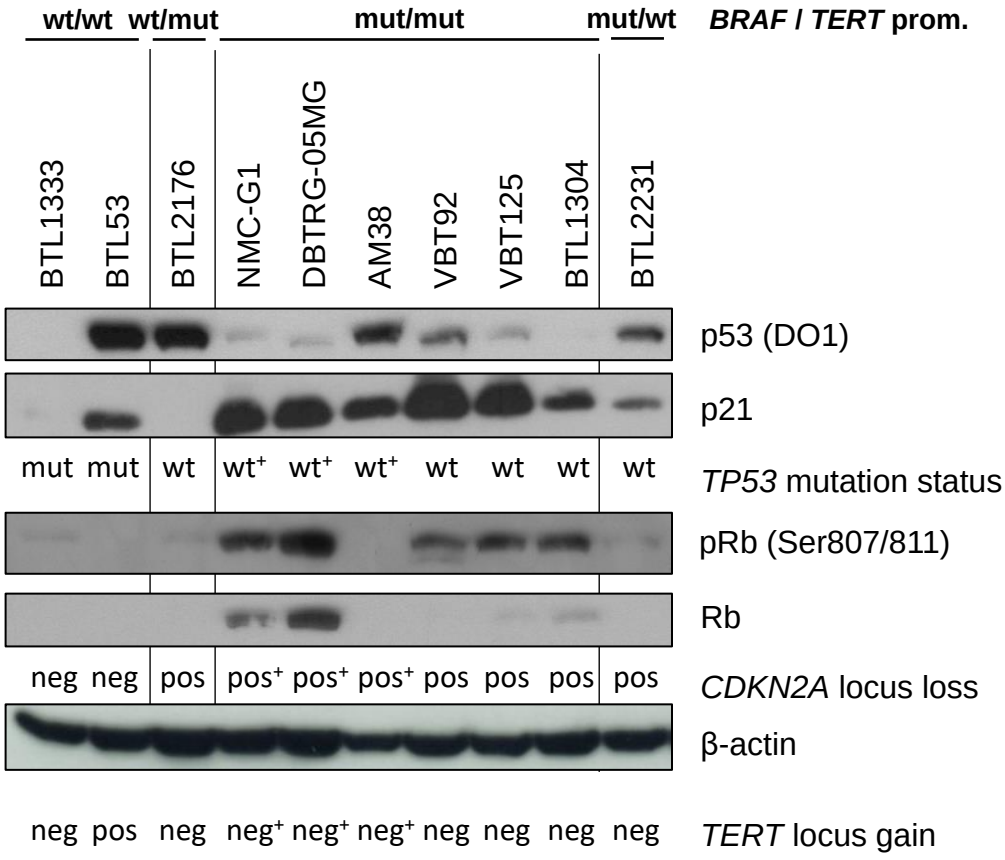

Figure S3. Evaluation of TP53 and CDKN2A/Rb signaling pathways. Protein expression of cell models with the indicated *BRAF* and *TERT* promoter status was analyzed by Western blot analysis. Additionally, *TP53* mutation status (hotspot mutations) and copy number variations of the *CDKN2A* and *TERT* locus are depicted. wt = wild-type, mut = mutated, $^{+}$ Source COSMIC database

Gabler et al., supplementary figure 4

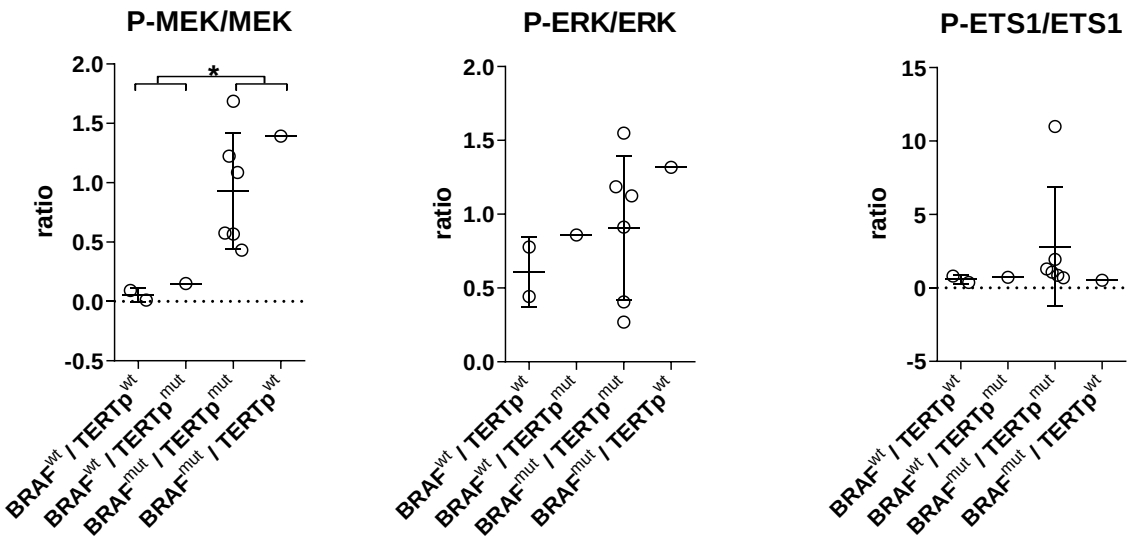

Figure S4. Activation levels of MEK, ERK and ETS1. Data are shown in different *BRAF* and *TERT* promoter genotypes as depicted. Activation changes are calculated from Western blot analysis by dividing the respective phospho-protein level by total protein expression normalized to beta-actin (compare Figure 1B). Values are given as mean +/- SD; Mann-Whitney test (two-tailed): BRAF wt (n=3) vs. BRAF mut (n=7), * p = 0.0167.

Gabler et al., supplementary figure 5

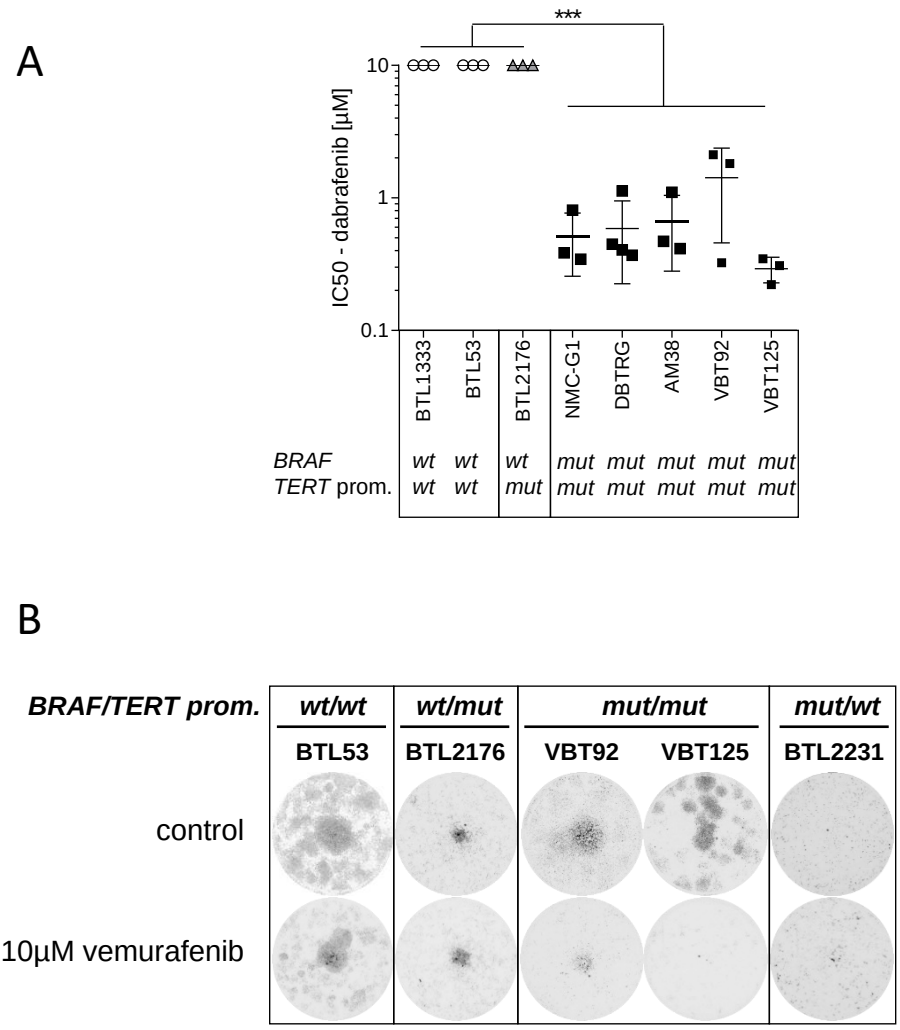

Figure S5. Anti-proliferative effects of BRAF inhibitors. **a)** Cytotoxicity assays were performed treating glioma cells of different *BRAF / TERT* promoter mutation status as depicted with dabrafenib for 72h. Values are given as mean +/- SD from three independent experiments. Ordinary one-way ANOVA (Tukey correction, 0.05 (95% confidence interval)), each *BRAF* wild-type versus each $BRAF^{V600E}$ mutated model: *** $p < 0.001$ **b)** Growth inhibition upon vemurafenib treatment. Clone formation assays for one *BRAF* wt/*TERT* promoter wt, one *BRAF* wt/*TERT* promoter mut, two *BRAF* mut/*TERT* promoter mut and one *BRAF* mut/*TERT* promoter wt cell model are depicted. Cells were seeded in duplicates in six-well format at low density and treated with 10µM vemurafenib for seven days. One representative well per condition is shown. wt = wild-type, mut = mutated

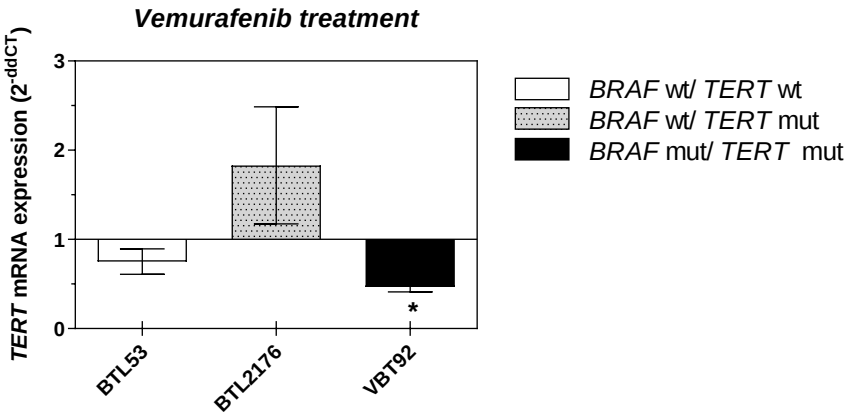

Figure S6. Inhibition of *TERT* expression upon vemurafenib treatment. mRNA expression of *TERT* was analyzed using qRT-PCR. mRNA was isolated from one *BRAF* wt and *TERT* promoter wt, one *BRAF* wt and *TERT* promoter mut and one *BRAF* mut and *TERT* promoter mut cell model as indicated. Cells were treated with 2.5µM vemurafenib for 16h. Results are shown as -ddCT (mean, +/- SD) from *RPL-41* serving as internal control and normalized to the respective untreated control. Unpaired student's t-test of controls vs. treatment wt = wild-type, mut = mutated

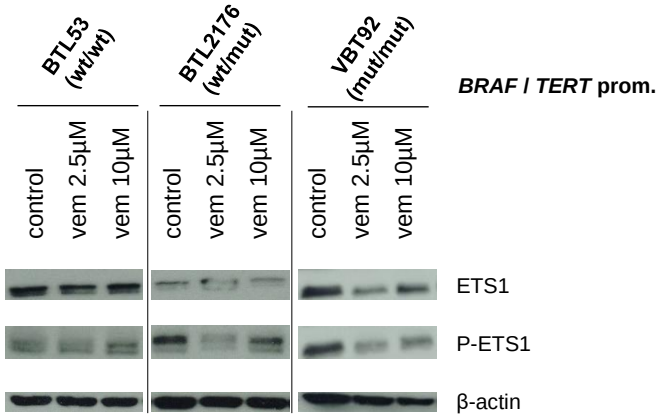

Figure S7. ETS1 inhibition upon vemurafenib treatment. Analysis of altered ETS1 phosphorylation upon 16h vemurafenib treatment by Western blot. β-actin served as internal control. wt = wild-type, mut = mutant, vem = vemurafenib

Gabler et al., supplementary figure 8

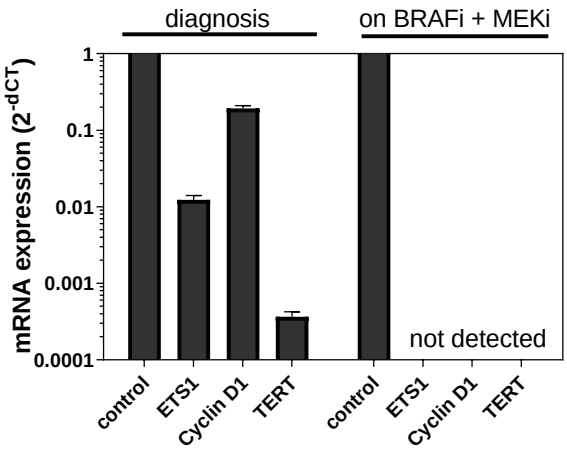

Figure S8. Changes in expression patterns in patient tissue upon targeted treatment. mRNA expression levels of *RPL-41* (control), *ETS1, cyclin D1* and *TERT* are shown. mRNA was isolated from the primary tumor (diagnosis) and from tumor tissue derived from a second operation during ongoing BRAF and MEK inhibitor (on BRAFi + MEKi) treatment. Values are given as 2^{-dCT} and normalized to *RPL-41* as internal control (mean +/- SD). BRAFi = BRAF inhibitor, MEKi = MEK inhibitor

Gabler et al., supplementary figure 9

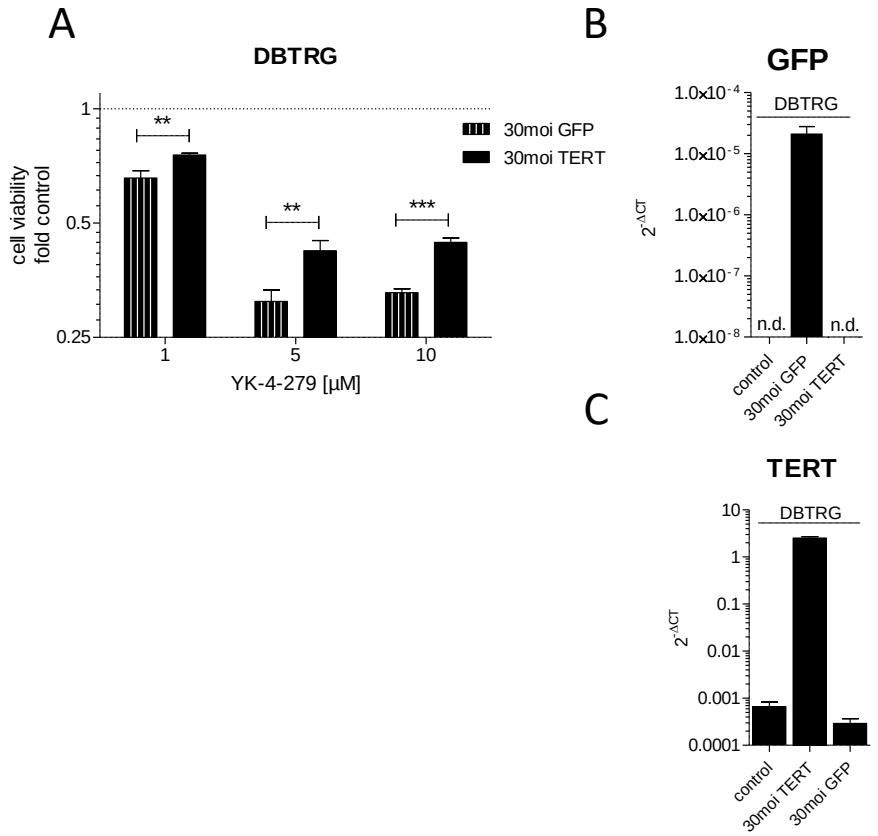

Figure S9. Ectopic *TERT* re-expression partly rescues double-mutant glioma cells from YK-4-279-mediated cytotoxicity. *BRAF^{V600E}/TERT* promoter-mutated glioma cells (DBTRG-05-MG) were infected with TERT adenovirus and the GFP adenoviral control at indicated moi. **(A)** Cytotoxicity assay with indicated concentrations of YK-4-279 was performed following virus infection. Values are given as mean +/- SD normalized to the respective untreated control, set to 1. (log2 axis, unpaired student's t-tests: **p<0.01, *** p<0.001) **(B+C)** qRT-PCR from the isolated mRNA was performed and revealed effective virus infection using both adenoviral constructs GFP (B) and TERT (C). Values are given as 2^{-dCT} from RPL-41 serving as internal control. moi = multiplicity of infection, n.d. = not detected, GFP = green fluorescent protein

Gabler et al., supplementary figure 10

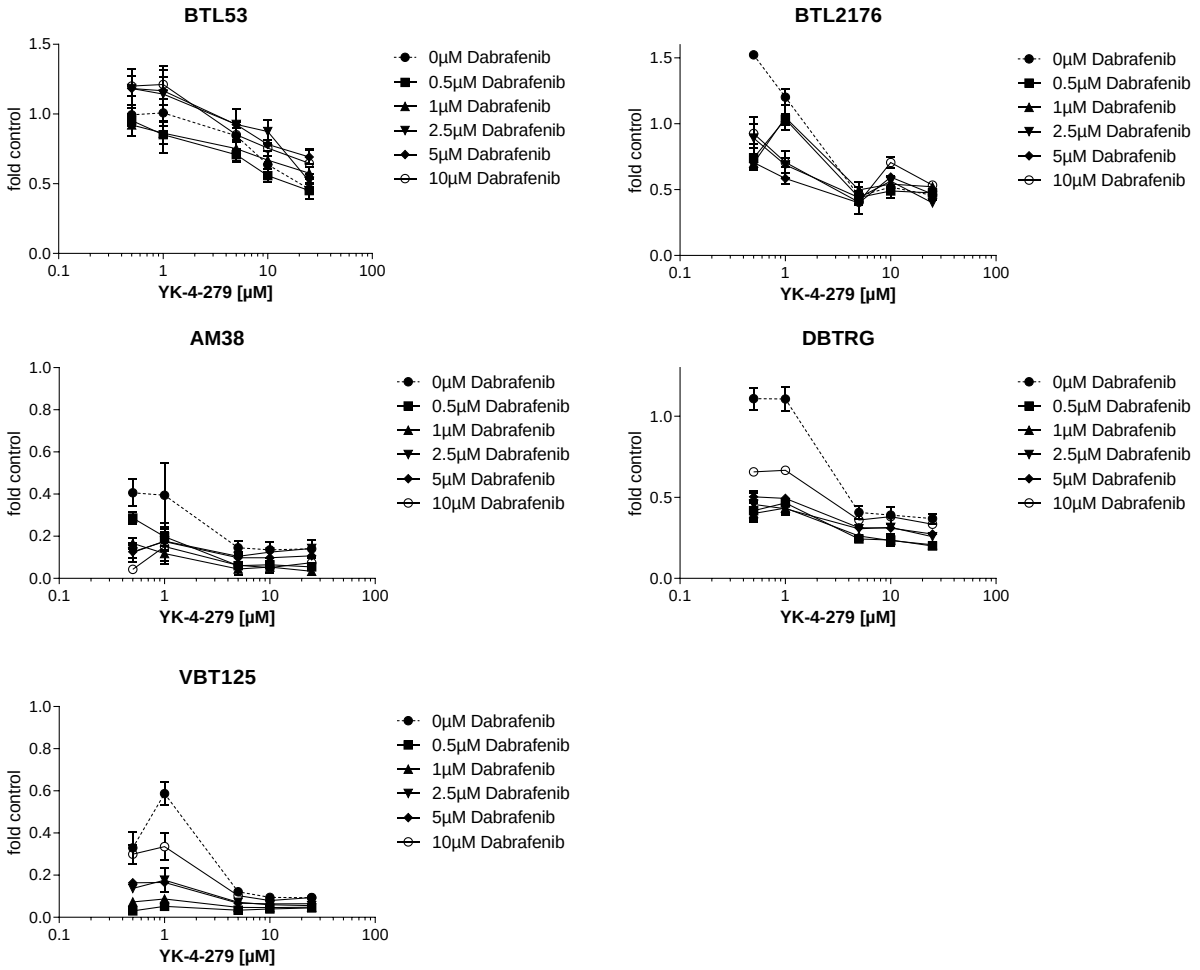

Figure S10. Combined BRAF and Ets-factor inhibition. Cytotoxicity assays were performed in cell models of different genotypes: *BRAF* wild-type / *TERT* promoter wild-type (BTL53), *BRAF* wild-type / *TERT* promoter mutant (BTL2176) and double-mutant (AM38, DBTRG, VBT125). Cell models were treated with combinations of dabrafenib and YK-4-279 for 72h. Values are given as mean +/- SEM from two independent experiments.